A friction model for use with a commingled fiberglass-polypropylene plain-weave fabric and the metal tool during thermostamping

Jennifer L. Gorczyca — James A. Sherwood — Julie Chen

University of Massachusetts Lowell
Department of Mechanical Engineering
Advanced Composite Materials and Textile Research Laboratory
One University Ave.
Lowell, MA 01854

JGorczyca@acmtrl.eng.uml.edu
{James_Sherwood, Julie_Chen}@uml.edu

ABSTRACT. *This research focuses on the friction mechanism at the tool/fabric interface during thermostamping of woven commingled glass-polypropylene plain-weave fabric. A friction model was derived after completing an experimental investigation into the effect of processing parameters on the steel/fabric friction mechanism. This friction model was incorporated into ABAQUS as a user subroutine for use with a finite element model of a thermostamping operation. Parametric finite element studies were conducted to investigate the effect of changing the binder-ring force and punch velocity on the reaction force of the punch during the thermostamping process. Punch velocity was found to have a much greater effect on the reaction force of the punch and state of strain in the fabric than the binder-ring force.*

KEYWORDS: *finite element analysis, thermoforming, woven-fabric composite material, friction.*

1. Introduction

Currently, the incorporation of composite materials into automotive and aerospace applications depends heavily upon a design-build-test methodology. Composite materials are desired because of their high strength-to-weight ratios, especially as both occupant safety and fuel efficiency (through decreased vehicular weight) are driving forces behind vehicle design today. However, the design-build-test methodology is high in cost, and it is not time efficient in comparison to the finite element technique.

If composite materials are going to be widely accepted for use in the production of automotive vehicles, then the parts manufactured using those materials must be capable of being made at essentially the same quality as the metal stampings they will be replacing without significantly increasing manufacturing cycle time or cost. Thermostamping of woven commingled composite fabrics is one manufacturing method that can potentially satisfy the high-volume, low-cost requirements without sacrificing quality. Thermostamped parts can exhibit the added benefits of weight reduction for increased fuel efficiency and of increased energy management during a crash situation when compared to their metal counterparts. It is believed that once the methods used to model the formation of a composite part are relatively accurate and well-understood, the resulting residual stress state and fiber orientations (or local material properties) will be available for modelling the deformation that a particular part will experience over a large range of strain rates, as in an automobile crash.

To facilitate the use of woven-fabric composite materials in this manufacturing process, a design tool should be readily available to assist design engineers in understanding and optimizing the complete thermostamping process. Such a design tool would reduce the reliance on the design-build-test methodology and decrease the time from the design stages to the production stages for a new composite part. As a result, manufacturers may be more willing to consider these new materials for use in their production vehicles.

This research focuses on the friction mechanism between the fabric and steel as part of that design tool. The results show that a friction model with the ability to change during the finite element modelling process based on the current processing parameters is important for inclusion in the design tool. The steel/fabric interface is under investigation because the punch, die and binder ring are all manufactured from steel and they are all in contact with the fabric blank during the thermostamping process.

(Dong *et al.*, 2000) performed a sensitivity study using explicit finite element analyses of dry-fabric hemisphere stamping and included Coulomb static friction at the punch/fabric and die/fabric interfaces for an eight-harness satin-weave fabric. The fabric was modelled as a solid continuum with anisotropic elastic properties. They studied the effects of friction, punch speed, shear and tensile moduli of the fabric and binder-ring pressure on the resulting shape of the stamped hemisphere by

comparing the shear deformation of the elements in their finite element models. To simplify their analyses, they neglected the friction at the binder-ring/fabric interfaces. Friction coefficients of 0.000, 0.125, 0.250, 0.375 and 0.500 at the die/fabric were examined with friction coefficients of 0.250 and 0.500 at the punch/fabric interface. The friction coefficients at all interfaces were constant during each simulation. Upon comparing the locations of maximum shear angle, it was noted that varying the friction coefficients in the manner described resulted in different deformation responses. For punch speeds ranging from 0.1 mm/s to 100 mm/s, they found no effect on the resulting shape of the hemisphere using their model. Large-scale changes in shear modulus had little effect on the deformation of the fabric around the punch. However, differences in fabric deformation were noted where the fabric was in contact with the flat surface of the die. Changes in tensile modulus did alter the deformation of the fabric. Low tensile moduli resulted in the fabric stretching more to conform to the shape of the die when compared to higher moduli. The amount of draw-in increased with increasing tensile modulus. Binder forces ranging from 22.8 N to 22.8 x 10^4 N resulted in similar deformations where the fabric contacted the punch and some differences where the fabric was in contact with the flat surface of the die. Numerical instabilities in the finite element analysis were noted for the largest binder force studied.

(Gearing *et al.*, 2001) studied friction at the tool/blank interface in metal stamping. Their study considered friction at the binder-ring/blank. *Via* a user-supplied friction subroutine in ABAQUS/Explicit, they incorporated an isotropic isothermal rate-dependent friction model into their finite element analysis. This rate-dependent phenomenological model was an extension of the model developed by (Anand, 1993) for implicit analyses. The model in the (Gearing *et al.*, 2001) study is for use with explicit analyses to take advantage of the faster processing times often associated with explicit analyses when compared to implicit analyses with surface interactions for large 3D models whose solutions are contact dependent. This model is robust enough to capture hardening and softening of the slip resistance with accumulated sliding distance under variable normal pressures. It was validated against experiments for cup- and square-pan drawing by comparing the reaction force on the punch from these experiments to the reaction force on the punch determined from their finite element simulations.

The current research differs from that of (Dong *et al.*, 2000) because it investigates the effect of a changing coefficient of friction on the results of finite element analyses of the thermoforming process. The coefficient of friction is updated for each Gauss point in each iteration of the analysis. In addition, this research differs from that of (Gearing *et al.*, 2001) because it focuses on fabric stamping as opposed to metal stamping and implicit analyses as opposed to explicit analyses.

2. Experimental

ASTM standards exist to determine the coefficient of friction of thin films. These standards consider the effects of normal load, temperature and pull-out speed on friction, but they do not take into account other influential factors in thermostamping structural composite sheets, *i.e.*, sheet viscosity and fiber orientation-factors which are important in the thermostamping of woven-fabric composite materials (Gorczyca *et al.*, 2004). For example, ASTM Standard D 1894 was designed for determining the friction of thin films, not woven fabrics, so this standard does not account for either sample orientation or fluid film viscosity. Using ASTM Standard D 1894 as a foundation, a friction test apparatus and test procedure were designed for the experiments used to develop the current friction model (Figure 1). This new test apparatus and associated procedure allowed for testing at various sample orientations and fluid viscosities for the plain-weave Twintex® fabric investigated in this study. The properties of this fabric are listed in Table 1.

When using woven commingled glass-polypropylene fabric, sample orientation is important because the direction of the tows could affect friction by altering the effective surface characteristics of the sample with respect to the steel tools. In addition, the respective tool and initial sample temperatures could also have an effect on friction through their effects on the viscosity of the polypropylene.

During thermostamping, a normal force is placed on the fabric by the binder ring. In the testing apparatus shown in Figure 1, the cam controls the pressure placed upon the fabric by increasing or decreasing the displacement between the steel pressure plates. The DC motor rotates the cam into position prior to the start of the test and thereby induces a pressure on the fabric. The speed reducer allows the speed of the motor to be controlled by the operator as the cam is rotated into position. The position of the cam remains constant during the test.

An LC703-1K 4448-N (1000-lb) tension-compression load cell attached to the fabric holder is aligned with the pulley and the fabric holder. It measures the load required to pull the fabric through the plates. An LCKD-1000 4448-N (1000-lb) pancake load cell is located beneath the bottom pressure plate and measures the normal force applied to the fabric. These load cells were obtained from Omegadyne, Inc. (Sunbury, OH USA).

During thermostamping, the fabric velocity is the rate at which the fabric slides along the metal tool. The velocity is affected by the shape and speed of the punch and the shear behavior of the tows. The deformation of the fabric as it conforms to the shape dictated by the punch and the die, through the shearing of the tows, can affect the speed at which the fabric slides between the binder ring and the die locally. Shearing will cause some portions of the fabric to lengthen and other portions to shorten. Thus, the fabric velocity will change with respect to location and point in time. Also, the velocity of the punch can potentially vary during the thermostamping process. A sample punch velocity profile obtained from Ford Research Laboratories (FRL) is shown in Figure 2 (Blanchard, 2004). Variation in

the punch velocity will also affect the fabric velocity as a part is being stamped. In the friction test apparatus used in this study, the fabric velocity is constant and controlled by an 1 127 Instron machine. Using this test apparatus, a single velocity value is investigated during each test. A compound-gear speed-multiplier system with a speed ratio of 10:1 allows testing to be conducted at speeds higher than those allowed by the Instron alone, 8.3 mm/s (Figure 1).
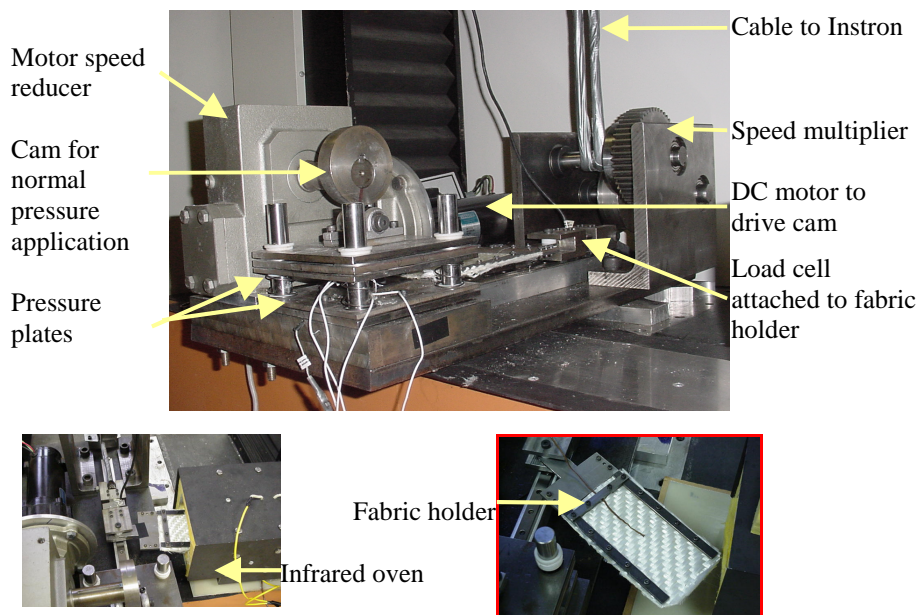

Figure 1. *Experimental apparatus for fabric friction experiments*

Table 1. *Twintex$^{®}$ plain weave fabric material input*

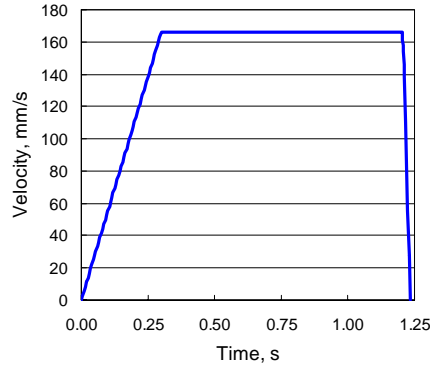| Property	Value
Initial tow width, w_0 (Liu *et al.*, 2004)	4.64 mm
Tow thickness, t (Liu *et al.*, 2004)	0.75 mm
Fabric thickness, H (Liu *et al.*, 2004)	1.5 mm
Initial inter-tow spacing, g_0 (Liu *et al.*, 2004)	0.75 mm
Glass content (mass) (Saint-Gobain, 2004)	60%
Glass content (volume) (Saint-Gobain, 2004)	35%
Melting point (Saint-Gobain, 2004)	165°

Figure 2. *Velocity profile for punch in thermostamping process (Blanchard, 2004)*

Using this test apparatus, the friction coefficient can be calculated using Coulomb's Law,

$$\mu = \frac{F}{N} \quad [1]$$

where μ is the friction coefficient, and F is the pull-out force required to overcome the normal force, N. As this test fixture has two friction plates in contact with the fabric (top and bottom) during the test, Equation 1 is modified to give the effective coefficient of friction as,

$$\mu = \frac{F}{2 \cdot N} \quad [2]$$

where the factor 2 in the denominator accounts for the two faces of the fabric sample in contact with the friction plates.

To investigate the effects of the processing parameters on the friction coefficient at the metal/fabric interface, a set of baseline parameters was chosen. These baseline parameters were chosen because they represent the actual processing parameters (Blanchard, 2003) and because of prior research conducted by (Chow, 2002). Experiments were conducted varying one parameter at a time while holding all other parameters at their baseline values. Table 2 lists the various test parameters investigated along with the baseline values. Five samples were run for each set of parameters. Two layers of fabric comprised each sample. The friction-coefficient results were plotted versus the test parameter under investigation with error bars of one standard deviation.

Based on these experiments, it was concluded that velocity has the greatest effect on the friction coefficient, followed by tool temperature and normal force,

respectively (Gorczyca *et al.*, 2004). In addition, fabric orientation, initial fabric temperature and fabric bending have relatively no effect on the effective friction coefficient. After these conclusions were made, an investigation into an applicable friction model for use at the tool/fabric interface during thermostamping was conducted.

Stribeck theory was found to be applicable (Gorczyca, 2004). Using this theory, the coefficient of friction, μ, is plotted versus the Hersey number, H (Figure 3). As this theory is dependent on viscosity, relative velocity and normal load, it was a reasonable place to start for the study of friction at the interface of steel and a heated, commingled glass-polypropylene woven fabric. The Hersey number, H (Hutchings, 1992), sometimes referred to as the Stribeck number (Stachowiak and Batchelor, 2001) is a function of viscosity, η, speed, U, and normal load, N,

$$H = \frac{\eta \cdot U}{N} \qquad [3]$$

Because the Hersey number depends upon viscosity, a rheological model was necessary for the calculation of the Hersey number in Equation 3. The viscosity term was determined through use of the Power Law of Ostwald and de Waele,

$$\eta = m \cdot \dot{\gamma}^{n-1} \qquad [4]$$

where *m,* the consistency, and *n,* the Power-Law index, are temperature-dependent Power-Law parameters, and $\dot{\gamma}$ is the shear strain rate of the resin. The Power Law model was ultimately chosen as the rheological model to incorporate into the Hersey number calculations because the results from the experimental data obtained by Chow (2002) for a four-harness satin-weave commingled glass-polypropylene fabric matched the analytical results using that model best when compared to the results using the Bingham and Herschel-Bulkley models.

The shear strain rate, $\dot{\gamma}$, can be expressed as a function of relative velocity, *U*, and fluid film thickness, *h*,

$$\dot{\gamma} = \frac{U}{h} \qquad [5]$$

Substituting Equations 4 and 5 into Equation 3,

$$H = m \cdot \left(\frac{U}{h} \right)^{n-1} \cdot \frac{U}{N} \qquad [6]$$

where, for this research h = 0.07 mm, which was determined from optical microscopy for preconsolidated glass/polypropylene twill-weave samples by (Clifford *et al*., 2001).

Table 2. *Test parameters used for friction experiments*

Parameter	Baseline Value	Additional Values Investigated
Tool Temperature, ^{o}C	85	21, 70, 100, 120, 140
Fabric Temperature, ^{o}C	180	160, 200
Orientation, (^{o}Warp/ ^{o}Weft)	0/90	30/60, 45/45, 60/30, 90/0
Normal Force, N	1500	218, 343, 1000, 1069, 3000, 4000
Velocity, mm/s	16.6	1.66, 8.33, 41.6, 83.3
Fabric bending	Flat	S-Curve
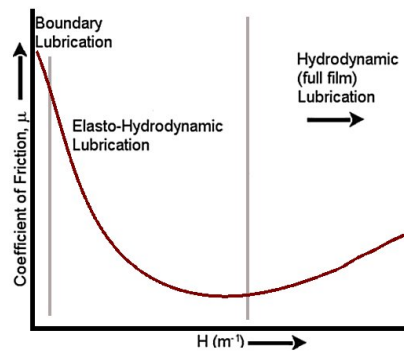
Figure 3. *Theoretical Stribeck curve (Hutchings, 1992)*

Equation 3 and Figure 3 imply that in this theory, the friction coefficient is dependent upon resin viscosity (melted polypropylene), fabric velocity (related to the stamping rate and tool geometry), and normal pressure (binder or punch force). It is important to recognize that the values for velocity and normal force in Equation 3 are test parameters that can be changed to give equal Hersey numbers (Figure 3). According to the Stribeck curve, equal Hersey numbers should result in equal friction coefficients. Multiple sets of experiments using different combinations of test parameters that generated equal Hersey numbers were conducted to demonstrate rigorously if the Stribeck relationship applies to the friction coefficient of a commingled glass-polypropylene woven fabric in contact with the steel tools

during the thermostamping process. Based upon these results, Stribeck theory was found to be applicable in all cases except for tool temperature. To account for tool temperature, a modification was made to the model through the inclusion of a shifting term. Thus, a friction model which includes the effects of the processing parameters on the friction coefficient existed for incorporation into the finite element code ABAQUS for conducting numerical simulations of the thermostamping process.

3. Numerical analyses

After incorporating the fabric friction model into the form required for the ABAQUS user friction subroutine, two sets of finite element analyses were conducted for this research. First, the fabric friction model was validated using a finite element model of the fabric friction test. Once it was concluded that the fabric friction model properly captured the phenomena noted from the experiments that were conducted, the friction model was used with a finite element model of the thermostamping process. At this point, a parametric study was conducted to investigate the effects of changing the binder-ring force and the punch velocity on the reaction force of the punch during the thermostamping process. Then, the need for a friction model which took into account a changing friction mechanism based on the current conditions of the fabric was assessed for inclusion in predictive finite element models of the thermostamping process.

3.1. *Validation with friction-test finite element model*

Agreement was found between the experimental data and the friction-test finite element model for the baseline test conditions. Then, the test parameters in the finite element model were altered to ensure that the fabric friction model, based on the Hersey number, was working as the authors believed it should for a range of test parameters. The test parameters that were investigated in this part of the research were: velocity, normal force and tool temperature. The values for these test parameters used in this investigation are listed in Table 3.

One model was run for each parameter affecting the friction coefficient i.e. velocity, normal force and tool temperature. The combinations of test parameters were chosen to ensure that both an increase and a decrease in friction coefficient would be investigated. Increasing the velocity will increase the friction coefficient, and increasing the normal force or increasing the tool temperature will decrease the friction coefficient. The results from these models are shown in Table 4. The percent differences are a consequence of the scatter within the data and the resulting equations from the regression analysis used to conclude the best-fit empirical model for all of the test data and the parameters that were varied from the baseline value.

Table 3. *Additional test parameters investigated – FE model of friction test*

Model	Velocity (mm/s)	Normal Force (N)	Tool Temperature (°C)
Baseline	16.67	1500 N	85
Vary Velocity	41.67	1500 N	85
Vary Normal Force	16.67	3000 N	85
Vary Tool Temperature	16.67	1500 N	140

Table 4. *FE model of friction test – Results*

Model	Experimental Friction Force (N)	Numerical Friction Force (N)	% Difference
Baseline	843	804	-4.5%
Vary Velocity	896	848	-5.3%
Vary Normal Force	1551	1673	+7.8%
Vary Tool Temp.	690	703	+1.9%

NOTE. — The numerical friction force was obtained from finite element simulations using fabric friction model and material model from (Li *et al*., 2004).

3.2. *Parametric study using thermostamping finite element model*

A parametric study was conducted using the thermostamping finite element model to investigate the effect of changing processing parameters on the reaction force of the punch. A material model, still under development by (Li *et al*., 2004), was used for this study. Unfortunately, there were no experimental data available for direct comparison of the numerical-simulation. Thus, the trends observed as a consequence of the change in friction due to varying processing parameters during the thermostamping simulations were studied and analyzed, as opposed to the actual values obtained from the thermostamping simulations. Section 3.2.1 will discuss the effect of changing the normal force applied by the binder ring on the reaction force of the punch and Section 3.2.2 will discuss the effect of changing the punch velocity on the reaction force of the punch. The reaction force on the punch is of importance because it is an indirect measure of the membrane forces in the fabric which in turn can be used ultimately to predict tow separation and breakage. Thus, relatively high reaction forces on the punch may indicate relatively high membrane stresses and tow separation and breakage as a result. This research does not yet address that issue in detail. It focuses on the change in reaction force on the punch.

3.2.1. *Parametric study of the effect of normal force*

Four models were run using the baseline displacement profile obtained from FRL (Figure 4). In these models, the normal force applied to the binder ring ranged from 650 N to 3000 N. These values span the range used in the thermostamping process (Chow, 2002; Blanchard, 2003; Peng, 2004). The reaction forces on the punch during the final forming step in the finite element model for each of the cases were compared. In Figures 5 and 6, it can be seen that the force required to stamp the part increases as the normal force on the binder ring increases.
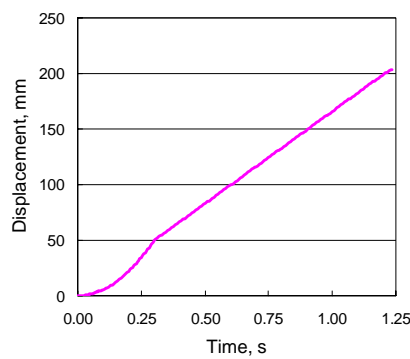
Figure 4. *Displacement profile for punch in thermostamping process at FRL (Blanchard, 2004)*
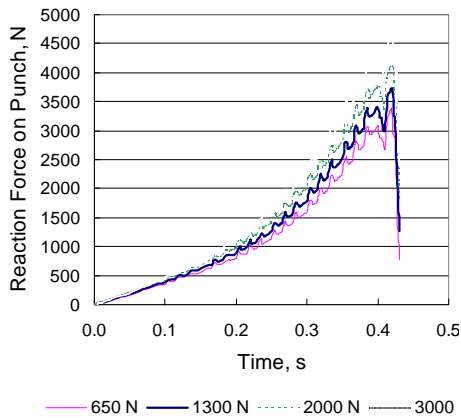
Figure 5. *Effect of increasing the binder-ring force on the reaction force of the punch*
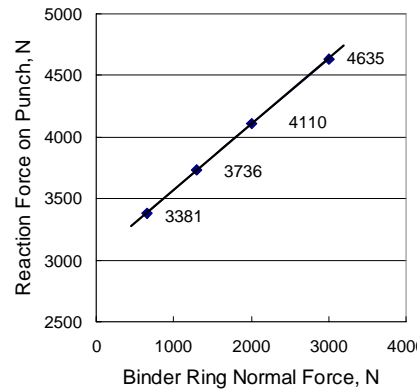
Figure 6. *Increase in maximum reaction force on punch for increasing normal force on binder ring*

This occurrence can be further explained in terms of the experimental data and with the aid of Coulomb's Law written in terms of the friction force, F, as,

$$F = \mu \cdot N \tag{7}$$

where μ is the Coulomb friction coefficient and N is the normal force. From Equation 7, for a constant friction coefficient, the friction force will decrease as the normal force decreases. However, the friction coefficient between the steel and the Twintex[®] used in this investigation is not constant for the test parameters studied. Based on the Hersey number and Stribeck theory, the friction coefficient is a function of normal force. Experimental data from the tensile friction tests showed that as normal force increases the friction coefficient decreases. Thus, Equation 7 can be rewritten as,

$$F = \mu(N) \cdot N \tag{8}$$

where μ (N) depicts the friction coefficient as a function of normal force, N. The increase in normal force is not proportional to the decrease in friction coefficient. In fact, according to the experimental data, the normal force increases faster than the friction coefficient decreases. Thus, the friction force is expected to increase as normal force increases, but the increase is nonlinear with respect to normal force.

The results from the numerical simulations exhibit the expected phenomena. As the pressure applied to the binder ring increases, the maximum force required to pull the fabric between the binder ring and the die increases linearly, as noted by the linear-regression trend line shown in Figure 6. The friction-test experimental data showed that for holding all other inputs constant, the coefficient of friction decreased as the normal force increased. Thus, during the thermostamping process, this increase in binder-ring pressure has a greater effect on the punch force required than the decrease in the coefficient of friction, which would result from an increase in normal force according to the fabric friction model used for this research.

In other words, increasing the binder-ring force to decrease the friction coefficient would not result in a decrease in the reaction force on the punch. The reaction force on the punch would increase due to an increase in the force required to overcome the higher normal force applied to the fabric. Decreasing the friction force would be desirable if fiber separation is occurring during the thermostamping process. However, increasing the normal force on the binder ring is not a way to decrease the friction force and reduce fiber separation and breakage. While increasing the normal force would decrease the coefficient of friction, the decrease is not enough to counter the increase in the membrane force in the fabric due to the increased normal force. This increased membrane force could result in fiber and/or tow breakage and separation.

3.2.2. *Parametric study of the effect of punch velocity*

The velocity of the punch will affect the rate at which the fabric slides beneath the binder ring and over the punch and die. In turn, the coefficient of friction where these components are contacting the fabric will vary according to the friction model, where increases in velocity will cause increases in the friction coefficient-for all other inputs remaining unchanged. As a result, an increase in the reaction force on the punch may occur as the velocity of the punch increases.

Three models were run in this investigation. A single model was run with the baseline displacement versus time profile obtained from FRL over a time increment of 0.43 s, the time it takes the punch to travel 70 mm and complete the stamping operation in the finite element model. The rate of this profile was decreased by 50% and increased by 100% in two subsequent finite element models as shown in Figure 7. The normal force on the binder ring was held constant at 650 N in each of these cases. It should also be noted that the punch is displacing at a relatively constant rate when it is in contact with the fabric. The rate changes only in the final 0.01 s based on the original profile obtained from FRL. However, the change in the rate of displacement of the fabric is varying continuously during the thermostamping process. Thus, the potential for changing fabric velocity must not be neglected in the friction model for use with the finite element method, as friction-test experiments showed that fabric velocity affected the friction coefficient.
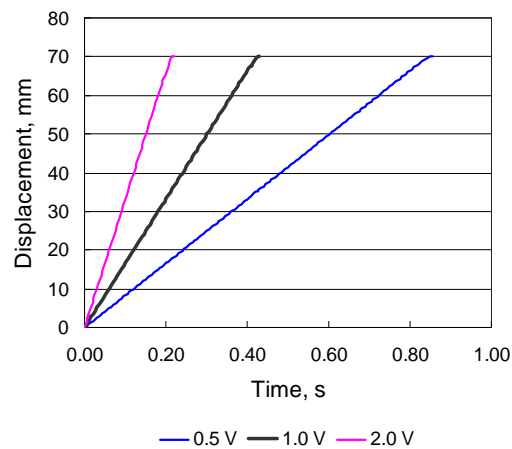

Figure 7. *Displacement versus time profile for punch used to prescribe the displacement of the punch for the baseline model (last 0.43 s), and the reduced and increased velocity models*

Figure 8 shows the reaction force versus time results for the three different punch velocity profiles examined in this research. Figure 9 shows the reaction force in terms of percentage of the stamping operation completed in the numerical model.

Increasing velocity has a nonlinear effect on the reaction force on the stamp. Figure 10 shows how increasing the velocity affects the maximum reaction force on the stamp. The x-axis indicates that the velocity profile obtained from FRL was decreased by one half (0.5 V), unchanged (V) and doubled (2.0 V). Figures 8, 9 and 10 also show that decreasing cycle time (*i.e.*, increasing the punch velocity) for the forming of a part will place additional force on the stamping tool. This increased force is only partly due to the change in friction coefficient as defined by the model proposed in this research and should be taken into account when designing thermostamping tools. Another cause for the increase in the reaction force on the punch will be discussed later in this section.
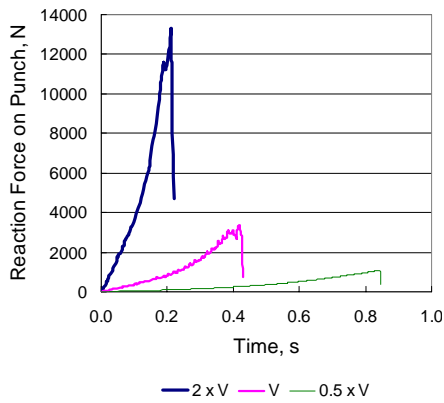
Figure 8. *Reaction force on punch versus time for punch-velocity parametric study*
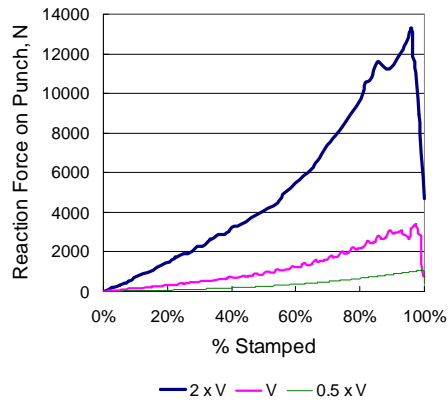
Figure 9. *Reaction force normalized by stamping step time in finite element model*
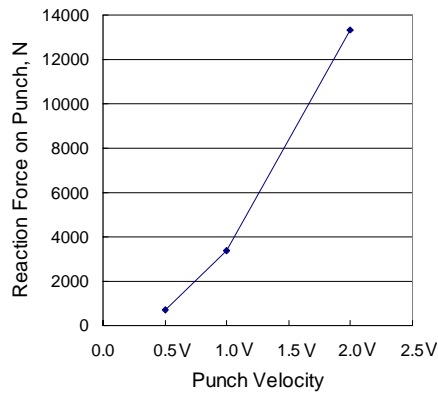
Figure 10. *Maximum reaction force on punch for punch-velocity parametric study*

In the fabric friction model, the friction coefficient increases as fabric velocity increases. As the punch velocity increases in the finite element model of the thermostamping process, the local velocity of the fabric sliding on top of the die and beneath the binder ring also increases. This increasing fabric velocity would result in an increasing friction coefficient. Thus, more force would be necessary to deform the fabric. It is therefore expected that an increase in punch velocity would cause an increase in the reaction force on the punch. It is not expected that this increase would be linear because the fabric velocity is raised to a power in the Hersey-number equation (Equation 6).

Additional numerical simulations were conducted because the increase in reaction force on the punch seemed high in this part of the study. First, the increase in reaction force on the punch with increasing velocity was examined using a friction coefficient of 0.3 in the default Coulomb friction model inherent to ABAQUS/Standard. Again, a nonlinear increase in the reaction force on the punch was noted with increasing punch velocity (Figures 11 and 12).
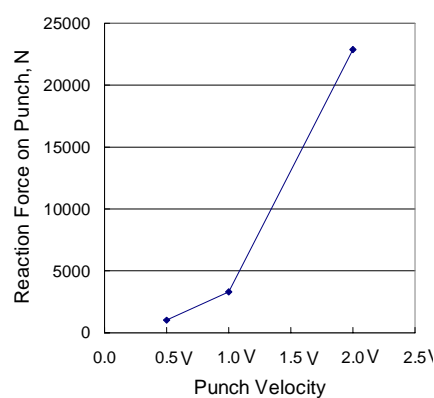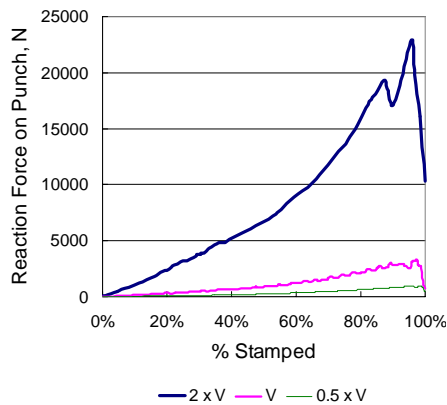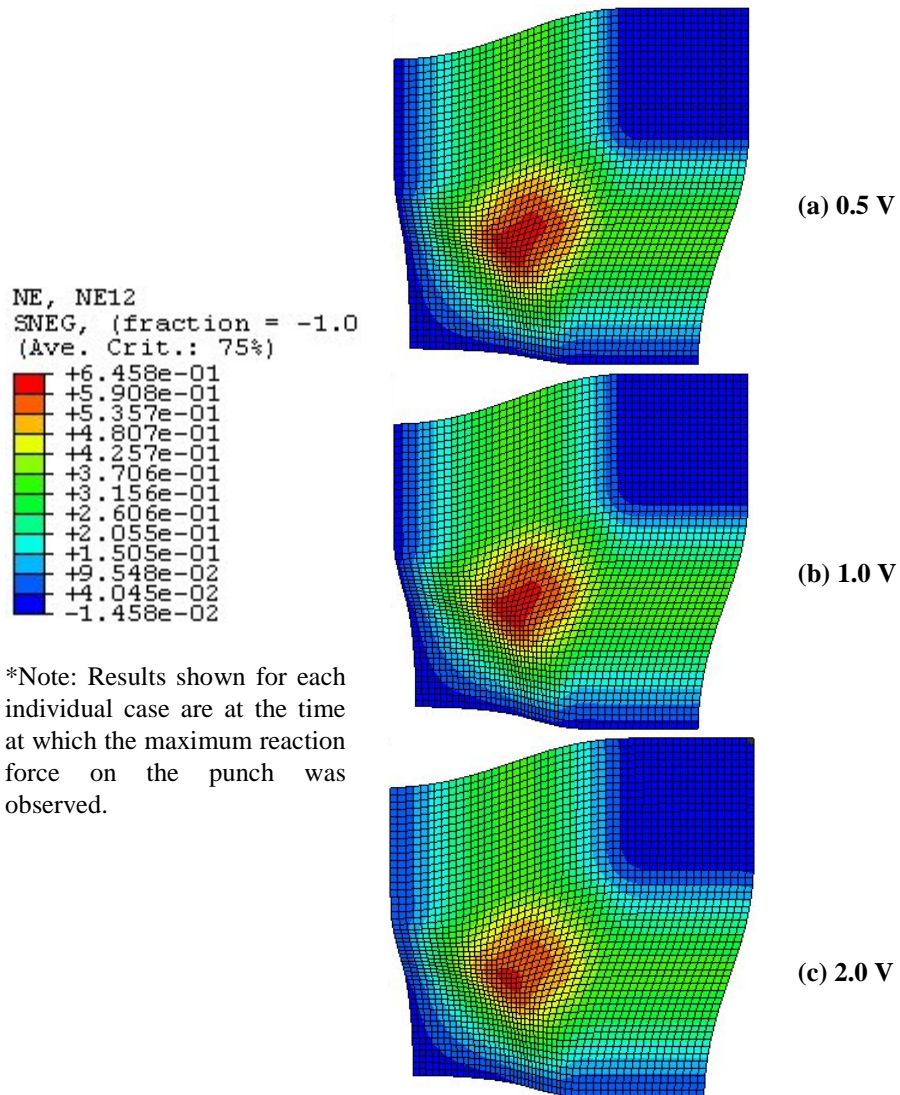

Figure 11. *Reaction force normalized by stamping step time in finite element model - Coulomb friction, $\mu = 0.3$*

Figure 12. *Maximum reaction force on punch for stamp-velocity parametric study - Coulomb friction, $\mu = 0.3$*

The change in the reaction force on the punch in this set of models is not equal to the change in the reaction force on the punch in the previous set of models where the fabric friction model based on the Hersey number was used. This result indicates that the punch velocity affects the reaction force on the punch whether or not there is velocity-based fabric friction model.
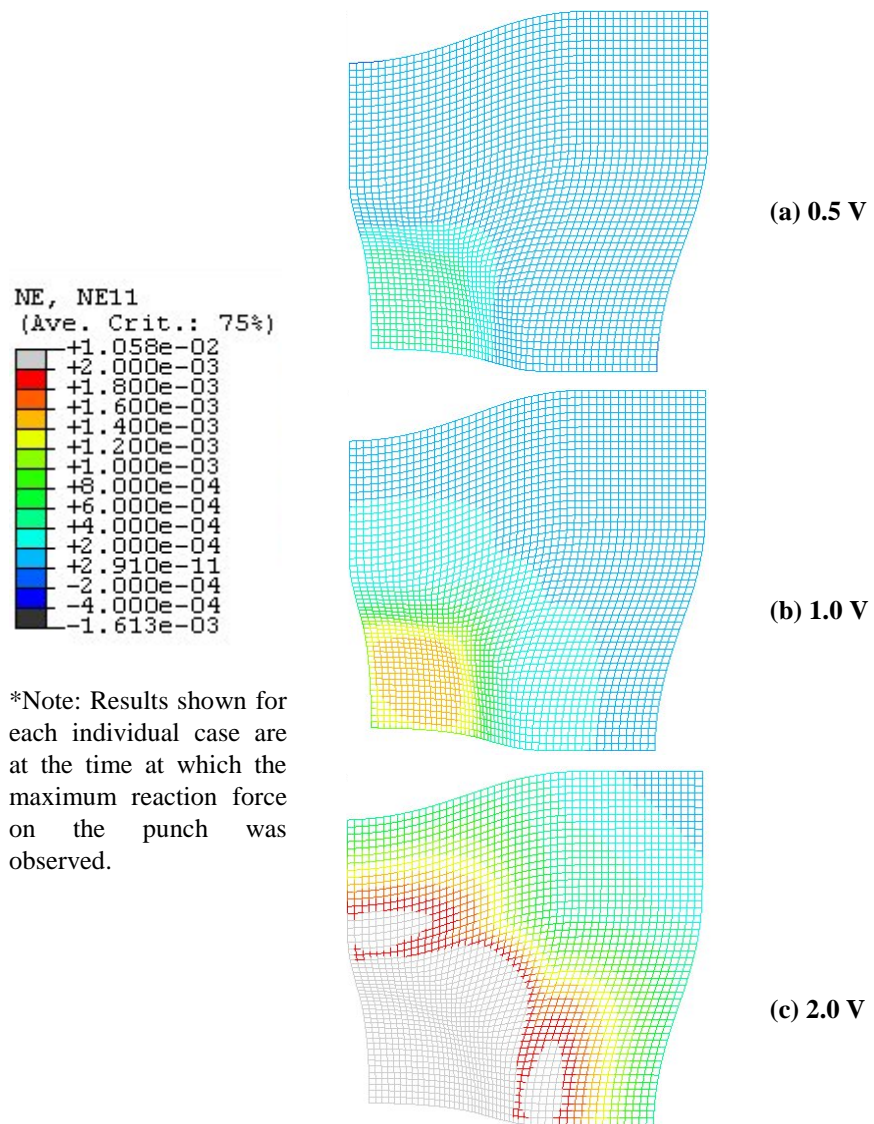
Next, using the three finite element models (0.5V, 1.0V, and 2.0V) with the Coulomb friction model ($\mu=0.3$), the shear strains of the shell elements were compared and the tensile strains of the truss elements were compared among the three sets of results. These comparisons were made at the time when the maximum

reaction force on the punch was calculated. Upon comparing the shear strains for the models with increasing punch velocity, it was noted that the increase in velocity caused the shear strain of the shell elements to decrease (Figure 13) and caused the tensile strain of the truss elements to increase (Figure 14).
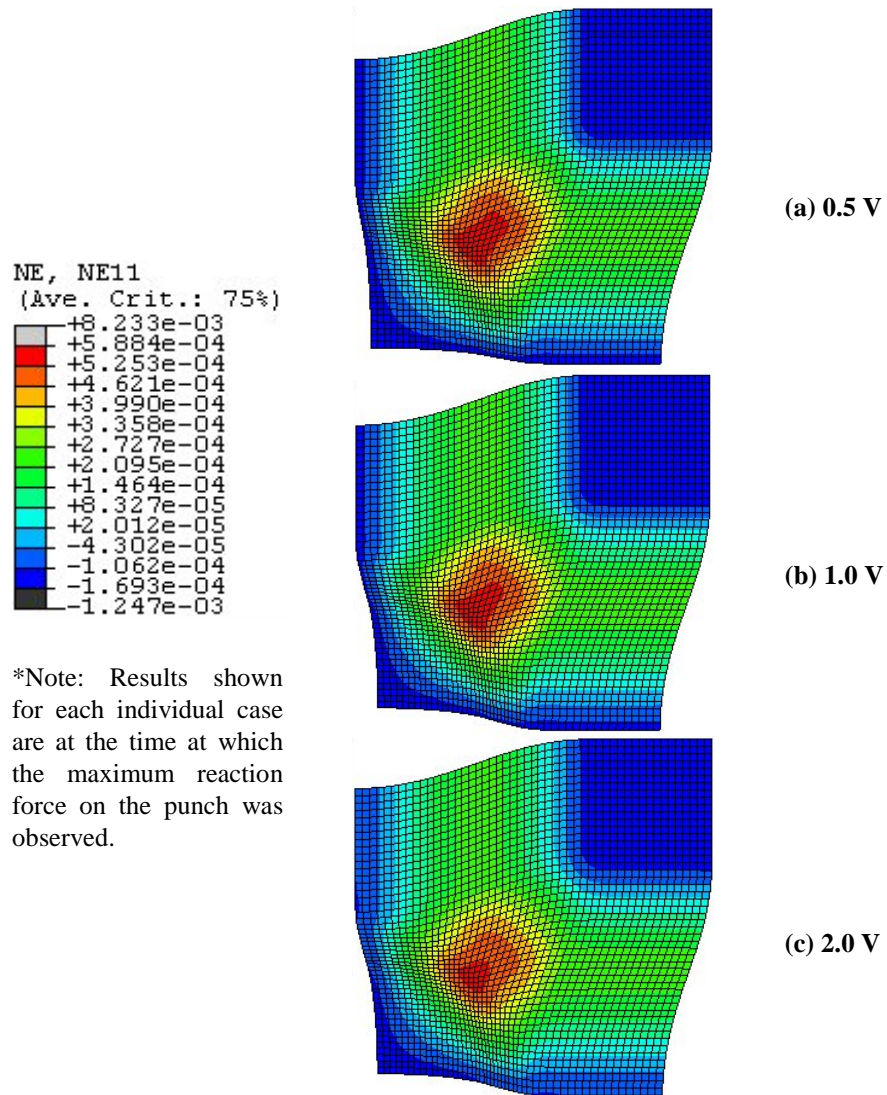


```
NE, NE12
SNEG, (fraction = -1.0
(Ave. Crit.: 75%)
    +6.458e-01
    +5.908e-01
    +5.357e-01
    +4.807e-01
    +4.257e-01
    +3.706e-01
    +3.156e-01
    +2.606e-01
    +2.055e-01
    +1.505e-01
    +9.548e-02
    +4.045e-02
    -1.458e-02
```

(a) 0.5 V

(b) 1.0 V

(c) 2.0 V

*Note: Results shown for each individual case are at the time at which the maximum reaction force on the punch was observed.

Figure 13. *Shear strain results for shell elements in thermostamping model using Li et al. (2004) material model and Coulomb friction with $\mu = 0.3$*

Figure 14. *Tensile strain results for shell elements in thermostamping model using Li et al., (2004) material model and Coulomb friction with μ = 0.3*

(a) 0.5 V

NE, NE11
(Ave. Crit.: 75%)
+8.233e-03
+5.884e-04
+5.253e-04
+4.621e-04
+3.990e-04
+3.358e-04
+2.727e-04
+2.095e-04
+1.464e-04
+8.327e-05
+2.012e-05
-4.302e-05
-1.062e-04
-1.693e-04
-1.247e-03

(b) 1.0 V

*Note: Results shown for each individual case are at the time at which the maximum reaction force on the punch was observed.

(c) 2.0 V

Figure 15. *Shear strain results for shell elements in thermostamping model using Li et al., (2004) material model and fabric friction model*
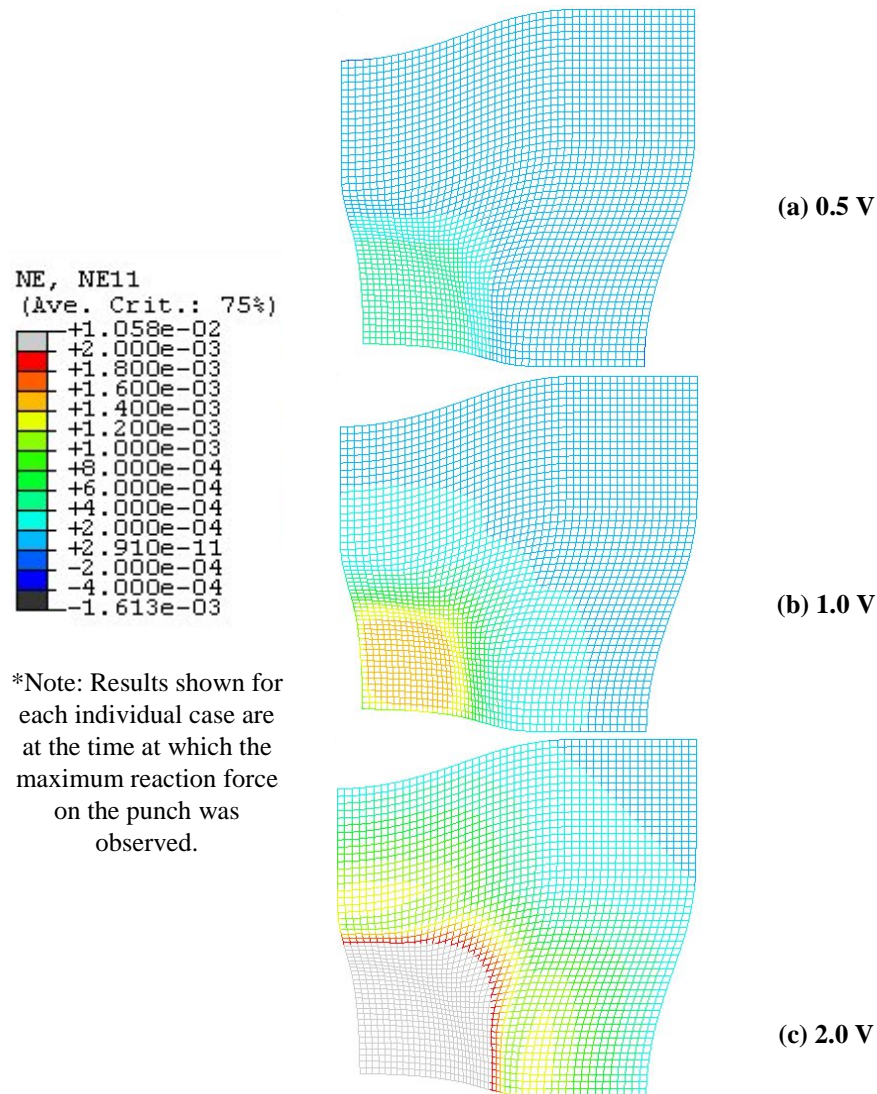
Figure 16. *Tensile strain results for shell elements in thermostamping model using Li et al., (2004) material model and fabric friction model*

Thus, it was not believed that the material model for the shell elements was the main cause of the increase in the reaction force on the punch with increasing punch velocity. The increase in tensile strain was believed to be the main cause for the increase in the reaction force on the stamp. The punch is trying to pull the fabric from beneath the binder ring faster than the fabric tows are able to shear and deform

to the shape of the punch. The tows are elongating thereby enabling the fabric to conform to the proper shape. As a result, the material model used for the truss elements which simulate the tows in the fabric is the source of the high reaction forces on the punch. The credibility of these reaction forces should be reinvestigated as the material model is refined.

To examine the shear and tensile strains using the proposed friction model, the results from another set of finite element models were examined. These models were identical to those run in the velocity study using the Coulomb friction model except the Coulomb friction model was replaced by the fabric friction model developed in this research. The effect of friction on the reaction force of the punch could be evaluated by comparing these new results with the results obtained using constant friction. Again, increasing velocity had only a slight effect on decreasing the shear strain of the shell elements at the time the maximum reaction force on the punch was reached (Figure 15).

Figure 16 shows the tensile strains. Like the results from the models with a constant friction coefficient, tensile strain increases with increased velocity. However the amount of this increase is different. To further investigate this occurrence, the reaction forces on the punch of the simulations run with the Coulomb friction model and the fabric friction model were compared.

In Figure 17a, using the baseline velocity profile obtained from FRL, note that the reaction forces on the punch are relatively equal. Upon examining this plot, one may think that there is not much need for a fabric friction model. However, changes in the reaction force of the punch are observed when the punch velocity is reduced by 50% and increased by 100%. As shown in Figure 17b, the predicted reaction force on the punch using the fabric friction model is higher than the predicted reaction force on the punch using the Coulomb friction model when the punch velocity is reduced by 50%, while the predicted reaction force on the punch using the fabric friction model is lower than the predicted reaction force on the punch using the Coulomb friction model when the velocity is increased by 100% (Figure 17c). This reversal in trends noted with increasing and decreasing punch velocities shows that the effect of processing parameters on friction should be incorporated into numerical simulations of the forming process. Research into the effect of these processing parameters on friction should be continued for incorporation into a truly robust design tool for the fabric forming process that will lead to the resulting residual-stress state. The resulting stress state could potentially influence the crash simulations of formed parts for the automotive industries.
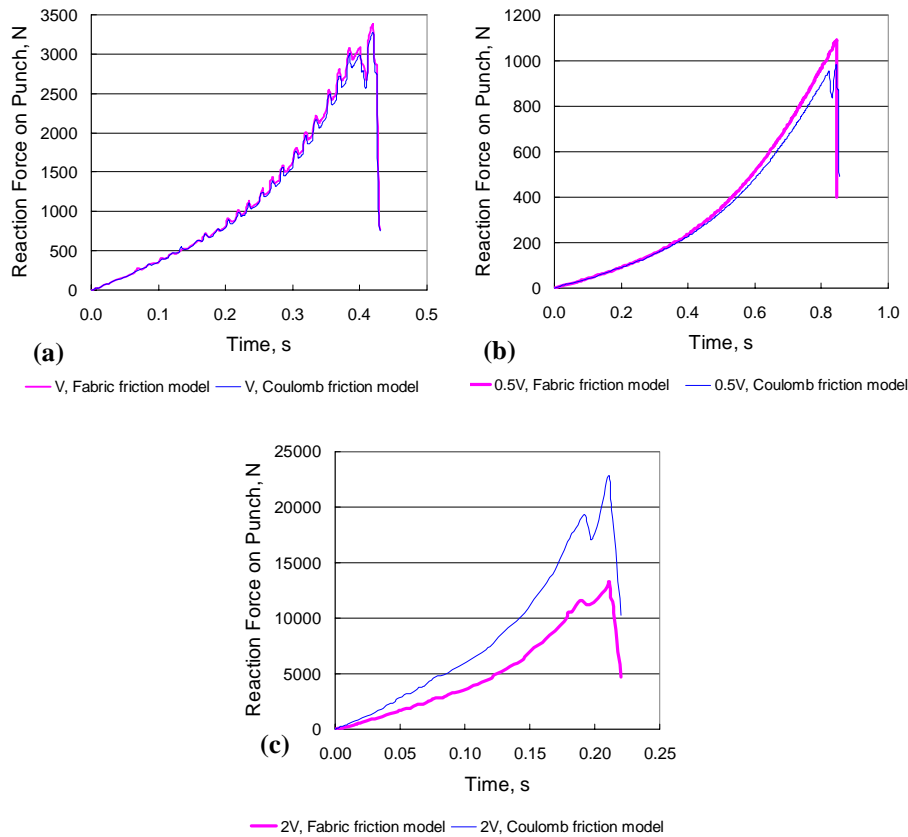
Figure 17. *Reaction force comparison between fabric friction model and Coulomb friction model (a) baseline V (b) 50% decreased V (c) 100% increased V*

4. Conclusions

The authors agree that the finite element model should be updated as the material model is refined. However, the trends noted in this study give insight into the importance of the continued development of an appropriate friction model for use in thermostamping simulations, especially when one of the goals is the development of a design tool.

A fabric friction model, developed in prior research, based on the Hersey number was used in this study. A parametric study was conducted using this fabric friction model with a material model for a commingled glass-polypropylene plain-weave fabric still under development by Li *et al.* (2004) in a finite element model of the thermostamping process. The results of this parametric study showed that increasing the velocity of the punch significantly increased the reaction force on the punch due

to the increase in the friction force at all metal/fabric interfaces. This increase in reaction force should be taken into consideration in the design of the thermostamping apparatus if low cycle times are ultimately desired. On the other hand, the increase in reaction force on the punch when the binder ring force is increased is due mainly to the net increase in tension in the fabric as opposed to changes in the friction coefficient. Increasing the force on the binder ring does not affect the reaction forces on the punch as greatly as increasing the velocity of the stamp. It is important to incorporate a friction model based on changing processing parameters into predictive numerical simulations otherwise the reaction force on the punch could be greatly overpredicted or greatly underpredicted. Over- or underpredicting the reaction force on the punch could compromise the predictive capabilities of numerical simulations using the finite element method. As a result, predictions of membrane stresses and the accompanying tow separation and breakage based on the numerically determined reaction force on the punch would be incorrect.

Acknowledgements

5. References

Anand L., "A constitutive model for interface friction", *Computational Mechanics*, Vol. 12, 1993, pp. 197-213.

Blanchard P., Ford Research Laboratory, Personal communications, Aug 2003 and Feb 2004.

Chow S., Frictional Interaction between Blank Holder and Fabric in Stamping of Woven Thermoplastic Composites, Master's Thesis, Department of Mechanical Engineering, University of Massachusetts Lowell, 2002.

Clifford M.J., Long A.C. and deLuca P, "Forming of engineering prepregs and reinforced thermoplastics", *2001 TMS Annual Meeting, Second Global Symposium on Innovations in Materials, Process and Manufacturing: Sheet Materials: Composite Processing*, (New Orleans, LA) 2001.

Dong L., Lekakou C. and Bader M.G., "Solid-mechanics finite element simulations of the draping of fabrics: a sensitivity analysis", *Composites Part A: applied science and manufacturing*, Vol. 31, 2000, pp. 639-652.

Gearing B.P., Moon H.S. and Anand L., "A plasticity model for interface friction: application to sheet metal forming", *International Journal of Plasticity*, Vol. 17, 2001, pp. 237-271.

Gorczyca J., Sherwood J. and Chen J., "Friction Between the Tool and the Fabric During the Thermostamping of Woven Co-Mingled Glass-Polypropylene Composite Fabrics", *Proceedings for the 18th Annual American Society for Composites Conference*, Gainesville, FL, October 20-22, 2003, paper number: 196.

Gorczyca J., *A Study of the Frictional Behaviour of a Plain-Weave Fabric during the Thermostamping Process*, Doctoral Dissertation, Department of Mechanical Engineering, University of Massachusetts Lowell, 2004.

Gorczyca J., Sherwood J., Liu L. and Chen J., "Friction and Shear in Thermostamping of Composites - Part I", *Journal of Composite Materials*, In Press, 2004.

Hutchings I.M., *Tribology: Friction and Wear of Engineering Materials,* CRC Press, Ann Arbor, 1992.

Li X., Sherwood J., Liu L. and Chen J., "A material model for woven commingled glass-polypropylene composite fabrics using a hybrid finite element approach", *International Journal of Materials and Product Technology*, In Review, 2004.

Liu L., Chen J., Gorczyca J. and Sherwood J., "Friction and Shear in Thermostamping of Composites - Part II", *Journal of Composite Materials*, In Press, 2004.

Peng X., Material Characterization and Stamping Simulation of Woven Composites, Ph.D. Dissertation, Department of Mechanical Engineering, Northwestern University, 2003a.

Saint-Gobain, Website: http://www.twintex.com/fabrication_processes/tw_process.html, 2004.

Stachowiak G. W. , Batchelor A. W., *Engineering Tribology,* Second Edition, Butterworth Heinemann, Boston, 2001.